COMPUTATIONAL REINVESTIGATION OF THE STRUCTURAL AND ELECTROLYTE PROPERTIES OF $Li_4P_2S_6$ AND $Na_4P_2S_6$

Yan Li and Natalie A. W. Holzwarth

Department of Physics, Wake Forest University, Winston-Salem, NC 27109, USA

Acknowledgements: NSF grant DMR-1507942 and WFU's DEAC cluster. Dr. Zachary Hood (MIT & ORNL) provided helpful discussions.

INTRODUCTION

Alkali-metal hexathiohypodiphosphate materials $Li_4P_2S_6$ and $Na_4P_2S_6$ are of interest to the effort of developing all solid state batteries. While, $Li_4P_2S_6$ has been found to have very small ionic conductivity[1-3] and is cited[4] as a decomposition product in the preparation of lithium thiophosphate electrolytes, $Na_4P_2S_6$ appears to be a competitive electrolyte for sodium ion batteries.[5] Recent experiments[5,6] have provided new structural and electrochemical results which have prompted reexamination of our earlier computational work on $Li_4P_2S_6$ and $Na_4P_2S_6$[1,7] to further understand its structural and conductivity properties. We also consider the possible mixed alkali electrolyte $Li_2Na_2P_2S_6$ which may have increased Na ion conductivity compared with that of $Na_4P_2S_6$.

MODEL STRUCTURES

Inequiv. Na(Li) P S

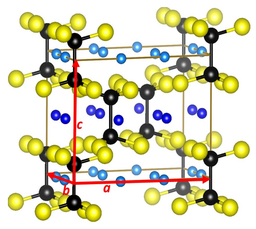

The Neuberger Structure

- Using a combination of NMR and X-ray measurement, the new experimental analysis by Neuberger *et al.*[6] on $Li_4P_2S_6$ concludes the structure to be ordered with space group P321 (# 150)
- Hexagonal structure with 36 atoms per unit cell (3 formula units)
- The building blocks $(P_2S_6)^{4-}$ ions are arranged in a pattern consisting of one third $\mathbf{P}_\uparrow$ and two thirds $\mathbf{P}_\downarrow$ placements
- The optimized structure is identified as having space group symmetry P$\bar{3}$m1 (#164) which is a supergroup of the space group P321

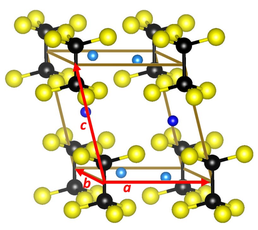

The Kuhn Structure

- The sodium ion material $Na_4P_2S_6$ was synthesized in 2014 by Kuhn *et al.*[8] and shown to be characterized by an ordered based-centered monoclinic structure with space group C2/m (# 12)
- Monoclinic structure with 12 atoms per primitive unit cell (1 formula unit)
- The layer arrangement of the $(P_2S_6)^{4-}$ units has 100% $\mathbf{P}_\uparrow$ placements
- Simulations by Rush *et al.*[7] using LDA suggested that the C2/m structure may be metastable with respect to lower energy configurations analogous to the $Li_4P_2S_6$ material
- Recent experimental results of Hood *et al.*[5] also find the C2/m structure

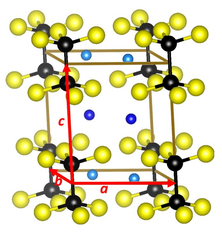

The Mercier Structure

- The crystal structure of $Li_4P_2S_6$ was analyzed by Mercier *et al.*[9] in 1982 finding a disordered lattice with space group $P6_3/mcm$ (# 193)
- The left diagram shows a subgroup P$\bar{3}$1m (#162) which corresponds to choosing all the P-P bonds of the $\mathbf{P}_\uparrow$ type
- Hexagonal structure with 12 atoms per primitive unit cell (1 formula unit)

COMPUTATIONAL METHODS

General

- Density Functional Theory (DFT) and Density Functional Perturbation Theory (DFPT) with the modified Perdew-Burke-Ernzerhof generalized gradient approximation (PBEsol GGA)[10]
- The projector augmented wave (PAW) formalism using ABINIT (https://www.abinit.org) & QUANTUM ESPRESSO (http://www.quantum-espresso.org)
- Datasets generated by ATOMPAW code available at http://pwpaw.wfu.edu

Static lattice and phonons calculations

- Calculations carried out by ABINT with $|k+G|^2 \le 50$ Ry
- Monkhorst-Pack k-point samplings of 6 ×6 ×8, 6 ×6 ×6 and 6 ×6 ×6 for the Neuberger structure, the Kuhn structure and the Mercier structure, respectively
- q-point meshes of 3×3×4, 3×3×3 and 3×3×3 for the above three structures in sequence

Ionic conductivity of $Na_4P_2S_6$ and $Li_2Na_2P_2S_6$ in the C2/m structure

- 2×1×2 supercell (96 atoms) constructed on basis of the conventional cell
- Calculations carried out by QUANTUM ESPRESSO with $|k+G|^2 \le 64$ Ry
- 2×2×2 k-point sampling of the Brillouin zone
- Migration energies evaluated using the implemented Nudged Elastic Band (NEB) Method[11]
- Molecular dynamics (MD) simulations performed using the microcanonical ensemble (NVE)

OPTIMIZED STATIC LATTICE STRUCTURES

TABLE I. Summary of static lattice results obtained using PBEsol GGA. Lattice constants for the primitive unit cells are listed in units of Å and angles in degrees. The energies ΔE are listed as eV/(formula unit) referenced to the energy of the P$\bar{3}$m1 structure.

$Li_4P_2S_6$	a	b	c	α	β	γ	ΔE
P$\bar{3}$m1 (#164)[a]	10.42	10.42	6.54	90.0	90.0	120.0	0.00
C2/m (#12)	6.08	6.08	6.89	97.9	97.9	119.1	0.31
P$\bar{3}$1m (#162)	6.03	6.03	6.48	90.0	90.0	120.0	0.04
$Na_4P_2S_6$	a	b	c	α	β	γ	ΔE
P$\bar{3}$m1 (#164)	11.10	11.10	7.25	90.0	90.0	120.0	0.00
C2/m (#12)[b]	6.51	6.51	7.52	98.5	98.5	117.6	0.00
P$\bar{3}$1m (#162)	6.45	6.45	7.13	90.0	90.0	120.0	0.09

[a] Corresponding experimental values quoted from Ref. 6 are $a = b = 10.51$ Å, $c = 6.59$ Å.
[b] Corresponding experimental values deduced from Ref. 8 are $a = b = 6.54$ Å, c = 7.54 Å, $\alpha = \beta = 98.7$ deg, $\gamma = 118.1$ deg.

STABILITY ANALYSIS

Fig. 1 shows the phonon dispersion curves along with the atom type projected density of states (PJDOS), comparing results for $Na_4P_2S_6$ in three considered structures. In each plot of bands, the path of high-symmetry q points is selected as recommended to the type of Bravais-lattice with corresponding diagrams shown in Fig. 1 (d) and (e). In view of the phonon frequencies throughout the Brillouin zone are real, each structure is predicted to be dynamically stable.

In order to understand the stability of each crystal structure, it's important to calculate the Helmholtz free energy F which is determined from the sum of the static lattice internal energy U_{SL} (based on DFT) and the phonon free energy F_{vib} (based on DFPT) due to lattice vibrations. Explicitly, the vibrational contribution F_{vib} is given by the equation,

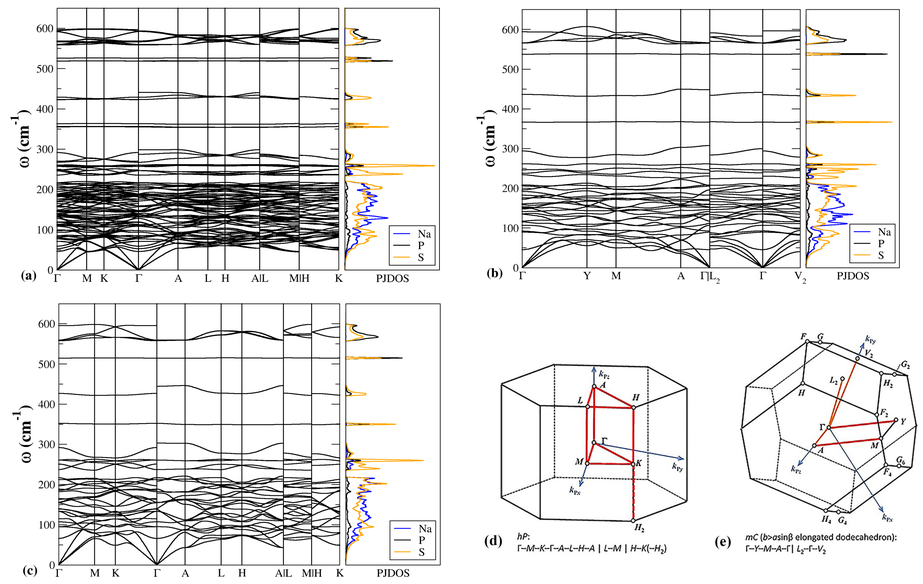

Fig. 1. Plots of phonon dispersion along with atom type projected density of states (PJDOS) for $Na_4P_2S_6$, comparing results in (a) P$\bar{3}$m1, (b) C2/m and (c) P$\bar{3}$1m structures. Brillouin zone diagram (d) for the P$\bar{3}$m1 and P$\bar{3}$1m structures and diagram (e) for C2/m structure are based on labels given by Hinuma *et al.*[12]

$$F_{vib} = k_B T \int_0^\infty d\omega \ln\left(2\sinh\left(\frac{\hbar\omega}{2k_B T}\right)\right) g(\omega)$$

where k_B is the Boltzmann constant and $g(\omega)$ represents the phonon density of states which is obtained by summing over PJDOS of each atomic species within the simulation cell. In practice, all results are evaluated within the approximation that there is no thermal expansion and the lattice vibrational frequencies are temperature independent.

In light of having lowest Helmholtz free energy as shown in Fig. 2(a), the C2/m structure is predicted to be the most stable structure of $Na_4P_2S_6$. Corresponding simulations for $Li_4P_2S_6$ indicate that it is stabilized in the P$\bar{3}$m1 structure. Overall, our results for structural stability of the two materials are consistent with the corresponding experimental analyses.[6,8]

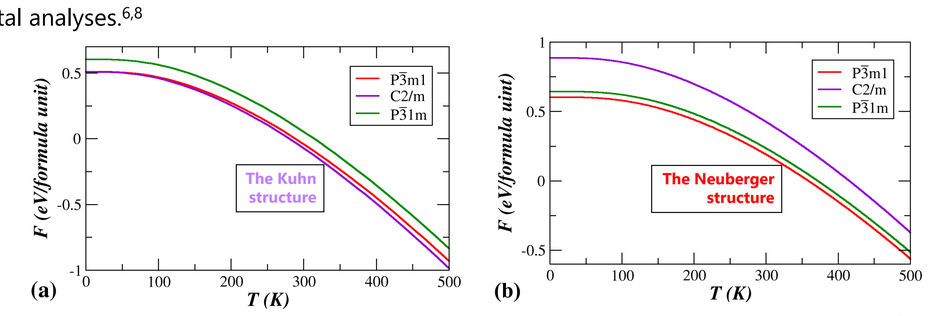

Fig. 2. Plot of Helmholtz free energy for (a) $Na_4P_2S_6$ and (b) $Li_4P_2S_6$, comparing results for the P$\bar{3}$m1 (red), C2/m (purple) and P$\bar{3}$1m (green) structures.

STABILITY OF $Li_2Na_2P_2S_6$

TABLE II. Energy changes in units of eV for the predicted reaction indicated by the first column, in which $Na_4P_2S_6$ is in the C2/m structure, metallic Na and Li are both in their bcc structures, and the lowest energy configuration of $Li_2Na_2P_2S_6$ is built from the C2/m structure of $Na_4P_2S_6$ by replacing Na ions of type g (light blue balls in the structural diagram) with Li ions. In the second and the third columns, we denote the corresponding static lattice energy difference $\Delta U_{sL} = U_{SL}^{right} - U_{SL}^{left}$ and the vibrational energy difference $\Delta F_{vib} = F_{vib}^{right} - F_{vib}^{left}$.

Reaction	ΔU_{SL}	ΔF_{vib} (T = 300K)
$Na_4P_2S_6 + 2Li \rightarrow Li_2Na_2P_2S_6 + 2Na$	-0.29	-0.06

The reaction energy is then estimated from $\Delta F = \Delta U_{sL} + \Delta F_{vib} + \Delta F_{elec}^{metal}$ which is shown in Fig. 3. Our calculation shows that the electronic contribution F_{elec}^{metal} from Na and Li metals is very trivial (~10^{-3} eV) that can be neglected.

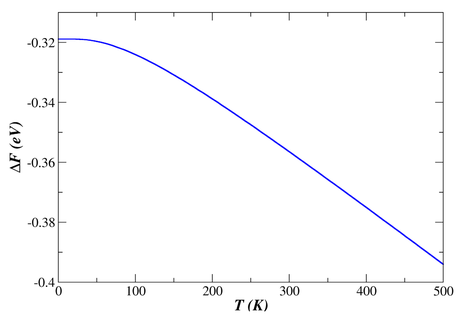

Fig. 3. Plot of the reaction energy as a function of temperature. Negative energies imply that the material $Li_2Na_2P_2S_6$ is stable with respect to the possible exothermic reaction.

SIMULATIONS OF Na ION VACANCY MIGRATION

The NEB results using the PBEsol GGA exchange-correlation functional indicate that the migration energy barriers E_m for Na ion vacancy diffusion between h sites to be the lowest with a value of 0.25 eV and 0.16 eV in $Na_4P_2S_6$ and $Li_2Na_2P_2S_6$, respectively. Due to the smaller migration and formation energies, the computed minimum activation energy E_A for Na ion conduction in $Li_2Na_2P_2S_6$ is less than that of $Na_4P_2S_6$ by 0.1 eV, which suggests $Li_2Na_2P_2S_6$ may be a valuable electrolyte material having better conductivity performance than $Na_4P_2S_6$.

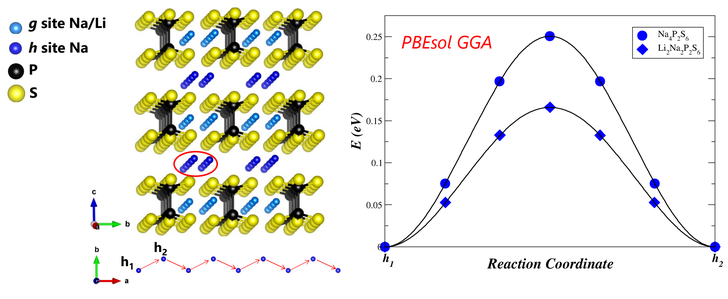

Fig. 4. Diagrams of energy path for Na ion vacancy diffusions in $Na_4P_2S_6$ (blue circle) and $Li_2Na_2P_2S_6$ (blue rhombus).

Activation energy: $E_A^{NEB} = E_m + \frac{1}{2}E_f$
where $E_f = E_{defect} - E_{perfect}$ is formation energy
Conductivity: $\sigma(T) = \frac{K}{T} e^{-E_A/k_B T}$

TABLE III. Comparison of activation energies E_A (eV) for Na ion migration in $Na_4P_2S_6$ and $Li_2Na_2P_2S_6$.

Material	E_A^{PBEsol}	E_A^{LDA} (Ref. 7)	$E_A^{Exp.}$ (Ref. 5)
$Na_4P_2S_6$	0.34	0.42	0.39
$Li_2Na_2P_2S_6$	0.23	--	--

SUMMARY

- According to PBEsol GGA results, $Na_4P_2S_6$ is to be stabilized in the C2/m structure and $Li_4P_2S_6$ is to be stabilized in the P$\bar{3}$m1 structure
- PBEsol GGA and LDA results of activation energy for Na ion migration reasonably agree with the experimental measurements which suggest $Na_4P_2S_6$ is a viable solid electrolyte
- Compared to $Na_4P_2S_6$, the mixed alkali electrolyte $Li_2Na_2P_2S_6$ can substantially enhances Na ion conductivity
- MD simulations are expected to provide more information on understanding the conductivity mechanisms

REFERENCES

[1] Z. D. Hood, C. Kates, M. Kirkham, S. Adhikari, C. Liang, and N. A. W. Holzwarth, Solid State Ionics **284**, 61 (2016).
[2] C. Dietrich, M. Sadowski, S. Sicolo, D. A. Weber, S. J. Sedlmaier, K. S. Weldert, S. Indris, K. Albe, J. Janek, and W. G. Zeier, Chemistry of Materials **28**, 8764 (2016).
[3] O. U. Kudu, T. Famprikis, B. Fleutot, M.-D. Braida, T. Le Mercier, M. S. Islam, and C. Masquelier, Journal of Power Sources **407**, 31 (2018).
[4] K. Minami, A. Hayashi, and M. Tatsumisago, Journal of the Ceramic Society of Japan **118**, 305 (2010).
[5] Z. D. Hood, H. Wang, X. Liu, A. S. Pandian, R. Peng, K. Keum, and M. Chi, An air-stable, water-processable, sodium thiophosphate solid electrolyte, to be published.
[6] S. Neuberger, S. P. Culver, H. Eckert, W. G. Zeier, and J. Schmedt auf der Gnne, Dalton Transactions **47**, 11691 (2018).
[7] L. E. Rush Jr. and N. A. W. Holzwarth, Solid State Ionics **286**, 45 (2016).
[8] A. Kuhn, R. Eger, J. Nuss, and B. V. Lotsch, Zeitschriftfr anorganische und allgemeine Chemie **640**, 689 (2014).
[9] R. Mercier, J. P. Malugani, B. Fahys, J. Douglande, and G. Robert, Journal of Solid State Chemistry **43**, 151 (1982).
[10] J. P. Perdew, A. Ruzsinszky, G. I. Csonka, O. A. Vydrv, G. E. Scuseria, L. A. Constantin, X. Zhou, and K. Burke, Physical Review Letters **100**, 136406 (2018).
[11] G. Henkelman, B. P. Uberuaga, and H. Jónsson, The Journal of Chemical Physics **113**, 9901 (2000).
[12] Y. Hinuma, G. Pizzi, Y. Kumagai, F. Oba, I. Tanaka, Computational Materials Science **128**, 140 (2017).